Case Studies in Thermal Engineering 76 (2025) 107306

Contents lists available at ScienceDirect

Case Studies in Thermal Engineering

journal homepage: www.elsevier.com/locate/csite

Multi-objective optimization of an industrialized wall system for sustainable housing

Carlos Rojas-Herrera [a], Aner Martínez-Soto [b,*], Rafael Batres [c], Rodrigo Cancino Carrasco [d], Natalia Reyes Barbato [e]

[a] *Facultad de Arquitectura, Construcción y Medio Ambiente, Universidad Autónoma de Chile, Av. Alemania 1090, Temuco, Chile*
[b] *Departamento de Ingeniería de Obras Civiles, Universidad de La Frontera, Av. Francisco Salazar 01145, Temuco, Chile*
[c] *Tecnologico de Monterrey, School of Engineering and Sciences, Prolongación Ezequiel Montes, Santiago de Querétaro, 76140, Querétaro, Mexico*
[d] *Eagon Lautaro S.A, Ruta 5, km 644, Lautaro, Chile*
[e] *Centro Tecnológico para La Innovación en La Construcción, Arturo Prat, 1171, Santiago, Chile*

HIGHLIGHTS

- Optimized wall system cuts energy demand by 11.1 % in cold-climate housing.
- Industrialized modular design lowers carbon footprint and cost by 1.8 %.
- Assembly time is up to 8 × faster under controlled test conditions.
- Multi-objective method defines optimal insulation type and thickness.
- Wheat straw insulation offers best thermal and environmental results.

GRAPHICAL ABSTRACT

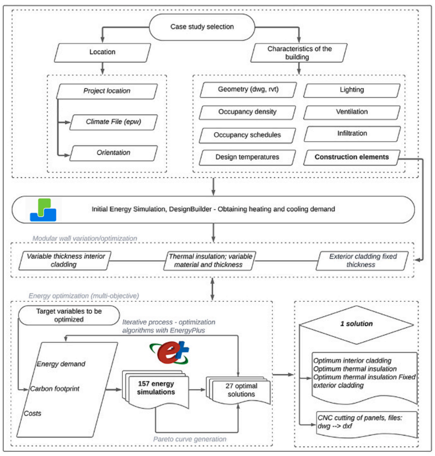

ARTICLE INFO

Keywords:
Industrialized construction
Energy demand

ABSTRACT

The construction sector is a major contributor to global energy consumption and greenhouse gas emissions, making it a central focus of sustainable development. Concurrently, the housing deficit has driven the adoption of industrialized construction systems in residential projects. This study

* Corresponding author.
E-mail address: aner.martinez@ufrontera.cl (A. Martínez-Soto).

https://doi.org/10.1016/j.csite.2025.107306
Received 9 June 2025; Received in revised form 9 October 2025; Accepted 23 October 2025
Available online 27 October 2025

WikiHouse
Thermal insulation materials
Assembly time

presents a multi-objective optimization of a modular wall system that integrates sustainability principles and alternative insulation materials to reduce energy demand for heating and cooling, carbon footprint, construction costs, and construction time. A workflow was developed, starting with the definition of a case study, including its location and architectural configuration for a cold climate, followed by dynamic energy simulations and optimization using evolutionary algorithms. A total of 157 simulations were conducted with DesignBuilder and EnergyPlus, assessing combinations of insulation materials (sawdust, wheat straw, and glass wool) and panel thicknesses. The optimal configuration included plywood panels and wheat straw insulation. Compared to a traditional wall, this solution achieved an 11.12 % reduction in energy demand, a 1.80 % reduction in carbon footprint, and a 1.80 % reduction in cost, along with a construction speed up to eight times faster under controlled test conditions. Additionally, when considering a more realistic heat pump scenario (CoP = 3), the operational carbon footprint decreases by approximately 66 %, reinforcing the environmental potential of the proposed system. These results demonstrate the capacity of optimized industrialized systems to deliver energy-efficient, low-impact, and scalable housing solutions, particularly in cold climates with urgent social housing needs.

1. Introduction

The construction sector represents one of the greatest challenges for global sustainability, as it is responsible for approximately 35 % of global energy consumption and 39 % of carbon dioxide (CO_2) emissions worldwide [1,2]. This issue is particularly critical in the residential sector, which accounts for 43 % greenhouse gas (GHG) emissions [3]. For instance, in cold-climate regions such as southern Chile, residential buildings have heating and cooling energy demands exceeding 230 [kWh/m^{2}year] [4], representing up to 53 % of total energy consumption [5].

In this context, the building envelope has become a key factor in reducing residential energy demand for heating and cooling [6]. Several studies have shown that improving the thermal performance of walls can reduce heating demand by up to 41 % and cooling demand by 47 % [7]. These reductions are largely attributed to the use of insulation materials with low thermal conductivity and high thermal inertia, which help stabilize indoor conditions and reduce reliance on active HVAC (Heating, Ventilation, and Air Conditioning) systems [8]. Among environmentally friendly materials that enhance building performance, lignocellulosic materials such as wheat straw and sawdust stand out. These are widely available byproducts from Chile's agricultural and forestry sectors. They exhibit thermal conductivities ranging from 0.034 to 0.048 [W/mK], along with higher densities that contribute to both thermal resistance and inertia [9,10]. Their application through blown-in insulation techniques [11] supports circular economy strategies and has been the focus of recent research on sustainable construction systems. These materials are suitable for integration into various construction systems, particularly within industrialized construction systems [12], which enhances sector productivity through modular or prefabricated systems, reducing construction time, minimizing waste, improving quality control, and increasing energy performance [13]. There is growing evidence of the benefits of industrialized construction in relation to the four key indicators of modern construction: cost, construction time, energy performance, and environmental impact [14].

Recent studies have shown significant advantages from applying multi-objective optimization strategies to building design. For example, improving the building envelope in single-family homes has been shown to reduce heating consumption by up to 30.4 % by lowering façade U-values from 1.81 to 0.91 [W/m^{2}K], with global energy savings of 9.17 % and annual CO_2 reductions of 162,8 [ktCO_2/year] [15]. In construction processes, the simultaneous integration of cost, time, and CO_2 emissions criteria has led to reductions of 20.95 % in execution time, 2.09 % in cost, and over 9 % in carbon emissions, while also improving perceived quality [16]. Other research incorporating time stochasticity has achieved global cost reductions while maintaining high schedule reliability (0.558–0.8) and quality levels above 0.9, demonstrating that balanced optimization of performance, cost, and time is attainable through intelligent system reliability-based strategies and evolutionary algorithms [17].

However, current literature lacks evidence on multi-objective optimization processes specifically focused on the main component of the building envelope (walls), and no clearly defined workflows have been proposed to address this approach. In addition, no studies were found that examine the practical aspects of industrialized components (such as walls or other constructive elements) regarding their performance in assembly and disassembly processes. While numerous optimization studies have explored energy performance or material selection, indicators of constructability or execution time are rarely integrated [18,19].

Moreover, the current market also lacks industrialized construction systems that simultaneously incorporate practical validation, bio-based materials, environmental, economic, and time-related sustainability criteria. Most existing studies address one or two of these aspects in isolation, without combining them into an integrated framework or applying them to cold-climate contexts with urgent social housing needs [20,21].

For these reasons, this study performed a multi-objective optimization [22] of an open-source modular wall construction system based on the WikiHouse concept, considering the four key indicators of modern construction: energy demand, carbon footprint, cost, and construction time. The optimization was carried out in DesignBuilder, which integrates evolutionary algorithms (NSGA-II) for performance-based building design. The WikiHouse system [23] is characterized by its prefabricated plywood structure cut with CNC technology, interlocking joint assembly, and high potential for low-cost replication, making it a relevant reference for affordable and sustainable housing solutions. The evaluation was conducted for a single-family social dwelling located in southern Chile, representative of cold-climate regions facing urgent energy and environmental challenges.

2. Methods

The general methodology was developed based on the identification of the case study, its geographic location, and the specific configuration of the evaluated dwelling. From these inputs, a baseline energy model was constructed to estimate heating and cooling thermal demand. Subsequently, the elements subject to optimization were defined: the interior cladding (variable thickness) and the thermal insulation layer (variable in type and thickness). The optimization process focused on three main objectives: energy demand, carbon footprint, and cost, using an iterative evolutionary algorithm to generate a Pareto front of non-dominated solutions. From this front, a representative configuration was selected and used to calculate and compare the energy, environmental, economic, and construction time performance indicators of the dwelling.

2.1. Case study and location

The evaluated model corresponds to a single-family home adjusted to the dimensions and construction logic of the WikiHouse modular system, specifically the Skylark 250 M type. This system uses CNC-cut structural plywood panels and allows for both conventional thermal insulation materials (such as glass wool) and alternative bio-based options (such as wheat straw and sawdust) [24]. The selection of this system responds to its increasing use in guided self-construction contexts and its adaptability to low-cost solutions with thermal efficiency. The base dwelling is derived from the work of Martínez-Soto (2021), who identified this model as the most replicated in the Chilean housing stock, according to the national residential energy end-use and conservation potential study [25].

Since cold regions account for the highest thermal energy demand in residential buildings [26,27], the case study was in the municipality of Lonquimay, in the Araucanía Region of Chile (geographic coordinates: 38°15′00"; −71°15′00″). This municipality presents climatic conditions comparable to those of Bergen (Norway), the Faroe Islands, Fiordland (New Zealand), and southern Chile, as all share a subpolar oceanic climate, characterized by cold, wet winters and cool summers, where temperatures rarely exceed 20 °C [28]. The geographic location and the influence of oceanic air masses result in a climate pattern with high annual relative humidity and pronounced thermal seasonality, creating a highly demanding scenario for the energy performance of the building envelope. For this reason, the specific climate of Lonquimay (classified as zone H under Chile's thermal zoning) was selected as the basis for the energy modeling of the case study.

2.2. Building characteristics

The base design of the case study considers a single-story dwelling with a total height of 2.40 [m]. Initially, the projected useable area was 58.20 [m^2]; however, to comply with the modular dimensions of the WikiHouse system, whose structural elements have a standard width of 0.60 [m], the layout was adjusted to 11.4 [m] in length and 7.4 [m] in width. This modification resulted in a total surface area of 63.0 [m^2], maintaining volumetric compactness and respecting the construction logic of the system. The dwelling analyzed is shown in Fig. 1, where (a) presents a rendered view and (b) shows the floor plan with the interior spatial layout.

The main parameters and input data used in the energy simulation model are summarized in Table 1. These include occupancy,

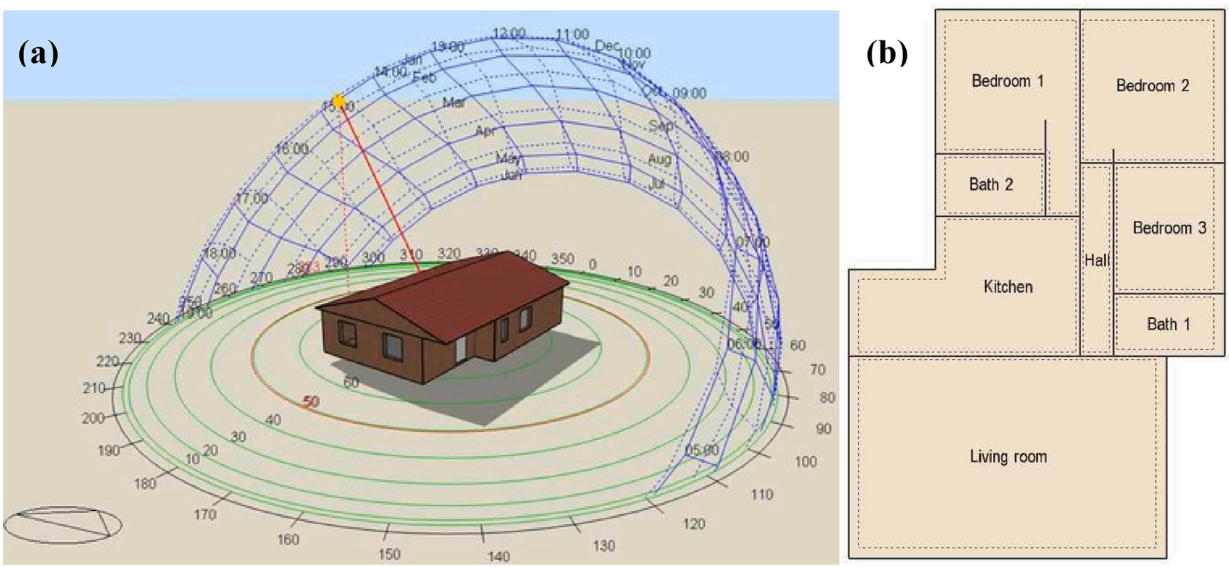

Fig. 1. Analyzed house: (a) rendered image, and (b) floor plan with interior spaces.

schedules, temperature setpoints, lighting, ventilation, and air infiltration rates. The information defines the baseline operational conditions for the dynamic simulations performed in DesignBuilder and EnergyPlus.

2.2.1. Construction elements

The configuration of the dwelling's construction elements was defined according to validated solutions and material assemblies compiled in Appendix A (Table A1). This appendix details the materials used in each component (walls, roof, floor, etc.), along with their thicknesses and total thermal transmittance (U-values). Notably, the element identified as "Modular Wall" (shown in Fig. 2) is the component subjected to energy optimization.

This wall features a multilayer composition arranged from exterior to interior as follows: an 18 [mm] exterior plywood panel, followed by a thermal insulation layer with three alternative materials (each analyzed with incremental thicknesses of 10 [mm]).

a) Sawdust, ranging from 150 to 250 [mm],
b) Wheat straw, ranging from 110 to 250 [mm],
c) Glass wool, ranging from 130 to 250 [mm].

Finally, an interior plywood panel of variable thickness was included, with options of 18, 21, 25, or 30 [mm]. The highest thermal transmittance value observed in this configuration corresponds to the least favorable scenario (sawdust insulation with 18 [mm] plywood panels on both sides), resulting in 0.288 [W/m^{2}K], which complies with the thermal requirements of the studied climate zone. This optimized modular wall element was also compared with a reference case using a traditional wall, to assess differences in thermal and environmental performance.

Fig. 2 illustrates the materials and configuration of the analyzed modular wall. In parallel, the remaining components of the dwelling's thermal envelope were defined according to validated construction solutions from Chile's Atmospheric Decontamination Plans (PDA) and the Ministerio de Vivienda y Urbanismo (MINVU). The adopted U-values were 0.29 [W/m^{2}K] for walls, 0.25 [W/m^{2}K] for the roof, 0.32 [W/m^{2}K] for the ventilated floor, 2.80 [W/m^{2}K] for windows, and 1.70 [W/m^{2}K] for doors. These values comply with the current Chilean thermal regulation for the cold-climate zone studied.

A detailed description of the composition, thicknesses, and material layers of each construction element, including the reference wall, roof, ventilated floor, windows, and doors, is provided in Appendix A, which compiles all construction specifications used for the thermal envelope of the case-study dwelling.

2.3. Multi-objective optimization

2.3.1. Energy simulation and optimization

The energy simulation was carried out using the DesignBuilder v7.3.0.029 graphical interface and the EnergyPlus v9.4 simulation engine, with the objective of estimating the dwelling's thermal behavior and annual heating and cooling energy demand. The model

Table 1
Summary of configuration and input data used in the simulation model.

Parameter	Description/Value	Reference/Source
Occupancy	5 occupants (two double bedrooms + one single). Occupancy density = 0.0794 [persons/m^2].	Model assumption
Schedules	Residential profiles (bedrooms, living-dining, kitchen, bathroom) from DesignBuilder defaults.	[29]
Temperature setpoints	Heating 20 °C/Cooling 24 °C (occupied); Heating 12 °C/Cooling 28 °C (unoccupied).	[30,31]
Lighting load	12 LED luminaires × 9.5 W = 1.81 [W/m^2], active during nighttime periods.	[32]
Ventilation	Qtotal = 0.015 × Afloor + 3.5 (Nbr + 1) → 14.95 [l/s] = 0.378 ACh.	NCh 3309:2014
Air infiltration	5 ACh (0.196 [m^3/s] total).	Chilean thermal regulation

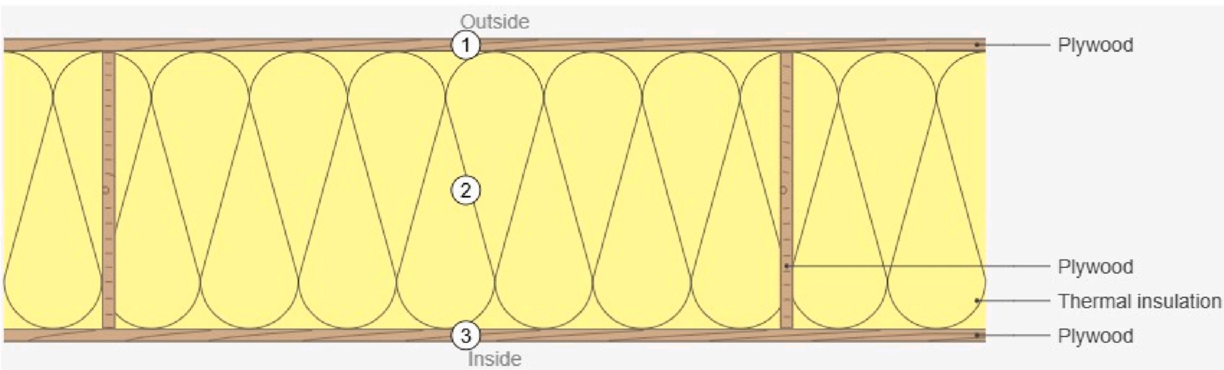

Fig. 2. Materials of the analyzed modular wall.

was built based on the previously defined geometry and configuration and was complemented with usage and operation data extracted from software default templates and local references appropriate for residential buildings in Chile. The output of each simulation included energy demand, material cost for the optimized wall, and the embedded carbon footprint.

A total of 157 simulations were conducted, covering all feasible combinations of insulation type and layer thickness. Specifically, three insulation materials were analyzed: sawdust (150–250 mm), wheat straw (110–250 mm), and glass wool (130–250 mm), each evaluated in 10 mm increments, together with four thickness options for the inner plywood panel (18, 21, 25, and 30 mm). This produced 156 unique configurations, plus one reference wall case used for comparison, resulting in a total of 157 simulation runs. The number of simulations ensured comprehensive coverage of the feasible design space, given the discrete and bounded nature of the decision variables, without requiring higher-resolution steps that would not significantly affect the Pareto-front shape or the relative ranking of optimal solutions.

The optimization focused exclusively on the wall assembly, which represents the largest portion of the building envelope and serves as the primary modular and structural component within the proposed industrialized system [33]. External walls typically account for the highest share of heat transfer through the envelope, ranging from 35 % to 45 % of total transmission losses, mainly due to their extensive exposed surface area and continuous interaction with outdoor conditions [34].

The optimization was performed using DesignBuilder's evolutionary algorithm, which follows the principles of the Non-Dominated Sorting Genetic Algorithm II (NSGA-II). The algorithm was configured with a population of 50 individuals and a maximum of 30 generations, with crossover and mutation probabilities of 0.9 and 0.1, respectively. Convergence was achieved when the Pareto front improvement remained below 1 % for five consecutive generations. These settings ensured a balance between computational cost and solution diversity, allowing an adequate exploration of the solution space. The number of iterations used in this study is comparable to that reported in research focused on the optimization of a single building component, which supports its validation against methodologies previously employed in the literature [35]. However, it is lower than in studies that incorporate multiple design variables, such as building orientation, roof configuration, or HVAC system selection, where the model's complexity requires a higher number of simulations to adequately explore the solution space [36].

2.3.1.1. Optimization considerations. The objective of the optimization process was to identify a modular wall configuration that simultaneously minimized: (i) the annual heating and cooling energy demand, (ii) the carbon footprint associated with the materials used, and (iii) the total construction cost. The optimization was performed using DesignBuilder's multi-objective optimization module, which applies an evolutionary genetic algorithm to generate the Pareto front. Although the software does not specify the exact algorithm, its behavior is comparable to the Non-dominated Sorting Genetic Algorithm II (NSGA-II), which is widely used in engineering multi-objective design problems [37]. Like NSGA-II, this approach enables the exploration of non-dominated solutions that balance energy efficiency, environmental impact, and economic cost [38,39].

The design variables considered included the type and thickness of the thermal insulation material (sawdust, wheat straw, and glass wool) and the thickness of the interior plywood panel in the modular wall. The objective variables defined in the software were: (i) Net site energy, (ii) total energy demand of the building (kWh/year), and (iii) CO_2eq carbon footprint (total emissions associated with the materials used and one year of building operation). Appendix B provides the unit cost and carbon footprint values of the main materials involved in simulation and optimization: plywood panels, sawdust, wheat straw, and glass wool. It also includes the corresponding data for the materials used in the traditional reference wall (OSB board, gypsum board, and EPS). All values are expressed as kilograms of CO_2 equivalent per kilogram of material (kgCO_2eq/kg) and unit costs per square meter or cubic meter, as applicable.

2.3.1.2. Optimal solution selection criteria. The selection of the final solution from the Pareto front was carried out through a combined approach, considering both the equity among objectives and their contextual relevance [40]. First, a central tendency criterion was applied [41,42], selecting the configuration with the minimum Euclidean distance to the origin in the normalized space of the three objectives: energy demand, carbon footprint, and cost. The distance D was calculated using equation (1):

$$D = \sqrt{(\widehat{f_1})^2 + (\widehat{f_2})^2 + (\widehat{f_3})^2} \tag{1}$$

where $\widehat{f_1}$, $\widehat{f_2}$ *and* $\widehat{f_3}$ are the normalized values of each objective function.

Additionally, a contextual prioritization criterion was incorporated, as in cold climates (such as the one defined in this study), the reduction of energy demand (EDD) has a direct impact on indoor comfort, CO_2 emissions, and overall cost. To reflect this priority, a weighted score model was applied, assigning a higher weight to the energy variable, as shown in equation (2):

$$S = 0.5 \times \widehat{f}dda + 0.25 \times \widehat{f}CO_2 + 0.25 \times \widehat{f}costo \tag{2}$$

2.3.2. Carbon footprint and construction costs

To estimate the carbon footprint and construction costs of the dwelling, the DesignBuilder software was used, as previously described in section 2.3.1. This tool includes an extensive database of physical properties, environmental impacts, and unit costs for a wide range of materials, which can be used directly or customized by the user. DesignBuilder allows energy simulation to be linked with life cycle assessment (LCA) and life cycle cost (LCC) analysis, integrating its engine with the One Click LCA platform, widely used in environmental impact studies of buildings [43]. In this study, the carbon footprint was estimated by considering two components: (i) the embodied carbon of materials, including extraction and transportation phases, and (ii) the operational carbon footprint, calculated from the heating and cooling energy demand over one year of use, assuming a fully electric resistance heating device with an efficiency (η) of 1.0 [44,45]. This assumption represents a conservative baseline scenario equivalent to direct electric resistance heating, allowing the influence of the envelope configuration on energy demand to be isolated without introducing variability from HVAC system efficiency. To complement this, a sensitivity projection was performed considering CoP values between 2 and 4, typical for electric heat pumps in residential buildings [46]. Under a representative value of CoP = 3, operational emissions would decrease by approximately 66 % compared to the baseline case, without affecting the relative ranking among optimized wall alternatives. Finally, total construction costs were calculated directly in the software by summing up the unit costs of all materials used in the complete building model [47]. These values represent only material costs, excluding labour, transportation, and other indirect expenses, since the analysis focuses on comparative differences among wall configurations rather than full life-cycle economic evaluation.

2.3.3. Assembly and disassembly time

To estimate the time required to construct the house using the optimized modular system, an experimental activity was developed based on the study by Bruno Bueno (2022), who analyzed the assembly times of the "Wall S″ module from the WikiHouse Skylark 250 system [48]. This system, which requires no mechanical fasteners, allows the inner wall thickness to be adjusted based on the type of insulation and is characterized by its ease of assembly and potential for part reuse. Given the hygroscopic behavior of wood-based panels such as plywood, with a moisture content between 10 and 12 % [49], a dimensional tolerance of 1–2 mm was incorporated in the design and CNC cutting stages to accommodate potential moisture-induced expansion or contraction induced by the relative humidity of the environment. All components were fabricated and assembled under controlled indoor conditions to ensure dimensional stability during testing.

The activity was conducted with five groups of second-year construction engineering students, selected to represent different levels of manual experience. Each group received a basic assembly guide (see appendix B) and participated in the full-scale 1:1 assembly and disassembly of a real wall module.

The following parameters were recorded during the exercise.

- Time for reading and understanding the instruction manual.
- Partial and total assembly and disassembly times, including interruptions, errors, and restarts.
- Qualitative observations regarding perceived difficulties, strategies used, and improvement suggestions.

A weighted average was calculated from this data, integrating results from all five groups. This allowed for the projection of the total estimated construction and disassembly time of the full house using the WikiHouse system. The projection assumed execution by a team of intermediate-skill users with no specialized tools. This activity was framed within a methodological approach for exploratory constructability validation, associated with Design for Assembly (DfA) strategies, which have been widely applied in the development and assessment of modular and prefabricated systems [50]. The participation of non-specialist users (such as students) allows for direct observation of accessibility conditions, assembly complexity, and logical sequencing, while also identifying potential barriers to real-world implementation in self-construction or progressive technical assistance scenarios. This type of testing has been proposed in

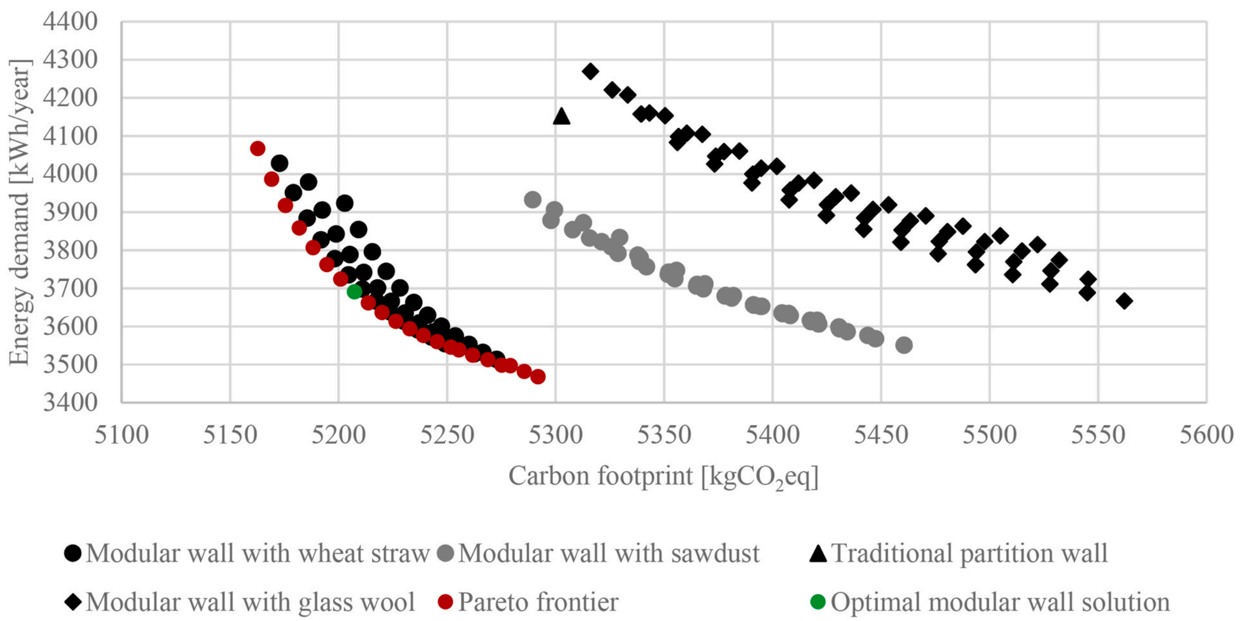

Fig. 3. Energy simulation results for 157 cases and generation of the Pareto curve with optimal solutions and identification of the optimal industrialized construction system solution.

literature as a useful tool to evaluate open-source systems like WikiHouse, whose constructive logic is based on digital fabrication and assembly without traditional mechanical fasteners [51]. It is important to note that the assembly times reported refers exclusively to the structural module and do not include complementary systems (electrical, plumbing, or finishing). Consequently, the results should be interpreted as indicative of assembly efficiency rather than complete construction productivity.

3. Results and discussion

3.1. Energy simulation and multi-objective optimization

The results of the energy simulation and the multi-objective optimization process are presented in Fig. 3, which shows a total of 157 evaluated scenarios and the resulting Pareto front, composed of 27 optimal solutions. These non-dominated solutions, shown in red, correspond exclusively to configurations using wheat straw as the thermal insulation material. The solution selected for this study, highlighted in green, achieves an energy demand of 3690 [kWh/year] and a carbon footprint of 5207 [kgCO_2eq], representing a favorable balance between thermal performance, environmental impact, and cost. In the central area of the figure, a group of solutions using sawdust can be seen, characterized by lower energy demand than other alternatives, but with a higher carbon footprint. In contrast, the solutions incorporating glass wool are grouped on the right side of the chart, showing higher levels of energy demand and carbon footprint compared to the other alternatives. The figure also includes the simulation result for the traditional timber wall, which lies outside the Pareto front, with lower thermal and environmental performance than the modular solutions, demonstrating its reduced overall efficiency.

The optimal solutions are primarily associated with the use of wheat straw as a thermal insulation material, which can be explained by its ability to achieve the lowest carbon footprint among the evaluated alternatives. This material exhibits the lowest thermal conductivity of the group, 30 % lower than sawdust and 21 % lower than glass wool, in addition to a density eight times higher than glass wool, although 35 % lower than sawdust [9]. This combination of properties enables strong thermal performance with low environmental impact, positioning it as a particularly effective option for cold climates [52]. In contrast, configurations using sawdust show higher carbon footprint results, although their energy demand is like that of the configurations on the Pareto front. This can be attributed to sawdust's high thermal storage capacity, reaching 93 [kJ/m^{2}K], nearly double that of traditional materials [10]. This property allows sawdust-based solutions to maintain energy demand levels comparable to those of wheat straw, despite their higher thermal conductivity. However, several studies indicate that in cold climates, such as the one considered in this study, low thermal conductivity has a greater influence on the overall energy performance of the envelope than the material's thermal inertia [53]. In fact, the energy demand variation range in sawdust-based configurations is narrower (9.7 %) compared to wheat straw-based optimal solutions (14.7 %), suggesting more stable thermal behavior, although not necessarily more efficient. While this effect is attributed to the material's thermal inertia, which performs better in warm climates, its usefulness in cold regions is more limited. Therefore, it is essential to select insulation materials according to the specific climatic context of each project. In this regard, sawdust may offer better performance than wheat straw in temperate or warm regions, where its thermal capacity can be more effectively utilized [54,55]. Table 2 summarizes the main thermal and physical properties of the insulation materials evaluated, highlighting the contrasts in conductivity, density, and thermal inertia that explain the differences observed in the simulation results.

3.1.1. Energy demand, carbon footprint, and costs

Table 3 presents a summary of the results obtained in terms of annual energy demand and carbon footprint for each of the simulated configurations of the industrialized wall system. The combinations are organized according to the thicknesses of the thermal insulation material (TIM) and the interior and exterior plywood panels (PP) of the modular wall. The results also include the traditional construction solution, which is used as a reference for comparison.

It is observed that the lowest carbon footprint is achieved in the scenario using wheat straw with minimum thicknesses (18/110/18 mm), while the lowest energy demand is obtained with the maximum thickness configuration (30/250/18 mm). In contrast, the glass wool scenario with minimum thickness (18/130/18 mm) results in the highest energy demand. The traditional construction solution shows a lower carbon footprint than three industrialized configurations: those using glass wool at minimum and maximum thicknesses (4.9 % and 2.98 % lower, respectively), and the one using sawdust at maximum thickness (0.26 % lower). However, in terms of energy demand, the traditional solution only outperforms the least efficient glass wool configuration, with a 2.74 % difference. This behavior indicates that, from an energy perspective, the optimal solution is the one with greater thicknesses, while from an environmental (embodied carbon) and economic (total cost) perspective, configurations with lower thicknesses are more favorable. This tension between objectives reinforces the need to apply multi-objective optimization approaches, which are widely used for the selection of

Table 2
Main thermal and physical properties of insulation materials used in the optimization.

Material	Thermal conductivity [W/mK]	Density [kg/m^3]	Specific heat capacity [kJ/kgK]	Thermal inertia [kJ/m^{2}K]	Relative CO_2 footprint [kgCO_2eq/kg]
Wheat straw	0.034–0.048	81	1.6	60	0.1
Sawdust	0.048–0.065	124	2	93	0.13
Glass wool	0.038–0.045	15	0.84	47	1.8

Table 3
Summary of energy simulation results.

Wall Configuration	Thickness [mm]	Energy Demand [kWh/year]	Carbon Footprint [kgCO_2eq]
PP/TIM(wheat straw)/PP	18/110/18	4066	5162
PP/TIM(glass wool)/PP	18/130/18	4269	5316
PP/TIM(sawdust)/PP	18/150/18	3932	5289
PP/TIM(wheat straw)/PP	18/180/18	3690	5207
PP/TIM(wheat straw)/PP	30/250/18	3467	5291
PP/TIM(sawdust)/PP	30/250/18	3550	5460
PP/TIM(glass wool)/PP	30/250/18	3666	5562
Traditional wall	According Table 1	4152	5302

integrated construction solutions [56], particularly in contexts with cost reduction and decarbonization targets for the housing sector [57,58].

The percentage variation between the maximum and minimum energy demand was 18.8 %, with the best performance corresponding to the configuration with wheat straw insulation and interior plywood at maximum thickness, and the worst to the configuration with glass wool at minimum thickness. This improvement range is consistent with the findings of Ouanès & Sriti (2024), who reported reductions between 13 % and 50 % in similar energy optimization scenarios. For carbon footprint, the variation between extremes was 7.2 %, in favor of the configuration with wheat straw at minimum thickness, compared to the most material-intensive case (glass wool + maximum panel thickness) [59].

In economic terms, the highest cost was estimated at USD 59,467, corresponding to the configuration with maximum thickness in both components. In contrast, the lowest cost was USD 58,401, associated with the scenario using minimum thickness. The difference between these two extremes represents a variation of approximately 1.80 %, indicating that cost has less relative dispersion compared to the other performance indicators. This low-cost variation shows that it is possible to significantly improve thermal and environmental performance with a relatively small increase in economic investment, which is attractive for implementation in housing policy frameworks.

3.1.2. Selection of the optimal wall system design

Among the configurations evaluated during the optimization process, two optimal solutions stand out, both combining 18 [mm] plywood panels with wheat straw insulation thicknesses of 170 [mm] and 180 [mm], respectively. This convergence of results is consistent with other multi-objective optimization studies, where the selected alternatives along the Pareto front tend to cluster around balanced configurations in key variables such as energy performance, which is directly related to operational costs and associated emissions [60,61]. This relationship is especially relevant considering that energy consumption and GHG emissions in the residential

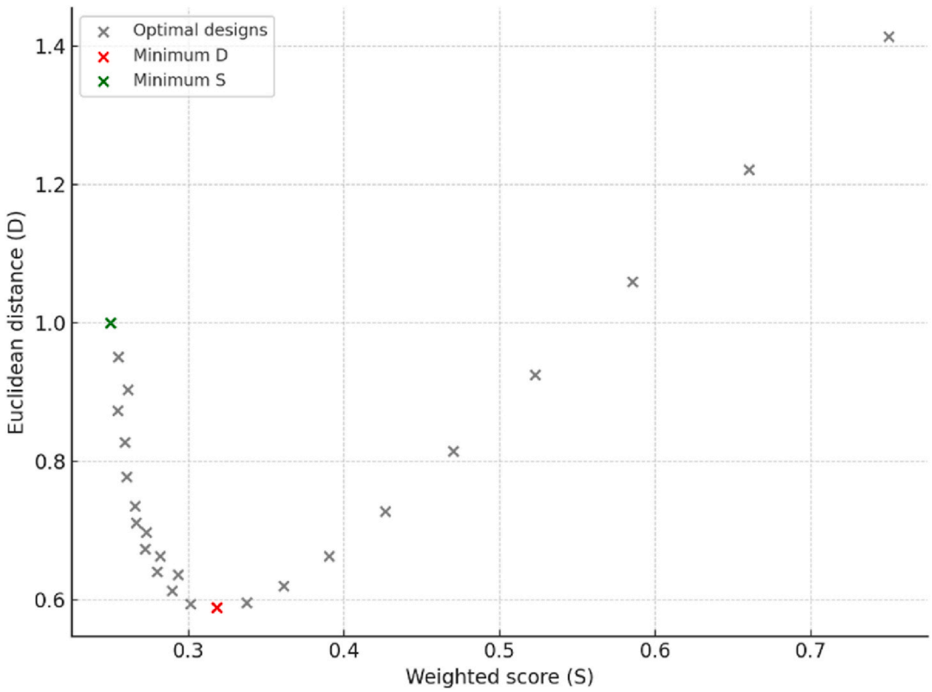

Fig. 4. Distribution of the optimal Pareto front solutions according to their weighted score (S) and Euclidean distance (D).

sector currently account for nearly 40 % globally, with unfavorable projections if no substantive action is taken [62]. Of the two alternatives mentioned, the configuration with 180 [mm] of wheat straw insulation achieves the lowest annual energy demand, with a value of 3690 [kWh/year]. Compared to the traditional timber wall solution, this industrialized alternative shows a reduction of 11.12 % in energy demand, 1.80 % in carbon footprint, and 1.80 % in total costs. For a typical social dwelling located in southern Chile, an 11.12 % reduction in annual energy demand represents a saving of approximately 250–300 kWh/year, equivalent to several weeks of winter heating. Achieving simultaneous reductions in energy demand, embodied carbon, and cost through a single design modification underscores the effectiveness of the multi-objective optimization approach, which balances environmental, economic, and constructive performance. In this sense, even moderate improvements at the material and component level can yield substantial cumulative benefits when scaled across large social housing programs.

Moreover, when comparing the 180 [mm] solution to the alternative with 250 [mm] of insulation (also with 18 [mm] plywood panels), the latter shows a slight improvement in energy demand, but at the expense of higher environmental and economic impacts: an increase of 6.00 % in energy demand, 0.86 % in carbon footprint, and 1.20 % in costs. Considering that the carbon and cost differences could be offset in the short term through energy savings, it is concluded that the 180 [mm] configuration represents an optimal balance point. The resulting wall assembly consists of two 18 [mm] plywood panels (interior and exterior) and a central 180 [mm] layer of wheat straw insulation, resulting in a total wall thickness of 216 [mm]. This configuration achieves a simultaneous reduction in energy demand, carbon footprint, and construction costs compared to the other alternatives analyzed. This selection was quantitatively supported through the calculation of two metrics applied to the Pareto front solutions: the normalized Euclidean distance (D) and the weighted score (S), as defined in section 2.3.1.2. The selected configuration, composed of 18 [mm] plywood and 180 [mm] of wheat straw, presented the lowest values for both metrics: $D = 0.5886$ and $S = 0.2960$, confirming its position as the most balanced alternative in terms of energy efficiency, environmental impact, and economic viability. Fig. 4 shows the distribution of these metrics across the evaluated optimal solutions.

Fig. 5 presents the construction detail of the optimized modular wall, showing the layout and thicknesses of its components. For this element, the embodied carbon footprint was calculated at 1.20 [kgCO_2/kg], representing a 56 % reduction compared to the traditional solution. Regarding cost, the value reached 20.23 [USD/m^2], which is 23 % higher than the traditional alternative; however, this increase is considered justifiable given the wall's thermal and environmental efficiency and its replication potential in sustainable solutions.

3.2. Case study results using the optimized construction system

3.2.1. Energy balance

Fig. 6 presents the annual energy balance of the dwelling using the optimized industrialized construction system, detailing the thermal losses and gains by building components.

In terms of energy losses, the component with the greatest impact is the glazing (windows), with 1570 [kWh/year], equivalent to 24 % of total losses. This is followed by the ventilated floor, with 1490 [kWh/year] (22 %), the walls with 1176 [kWh/year] (18 %), and the roof with 957 [kWh/year] (14 %). Ventilation accounts for 853 [kWh/year] (13 %), while air infiltration represents the remaining 636 [kWh/year] (9 %). These results highlight the importance of wall design and optimization, since despite having 46 % more surface area than the ventilated floor, the walls show 21 % less heat loss. Likewise, although wall losses are 19 % greater than those of the roof, this corresponds to the wall's 46 % larger surface area. Given the similar thermal transmittance values of these components, 0.25 [W/m^2K] for the roof, 0.29 [W/m^2K] for the walls, and 0.32 [W/m^2K] for the floor, the thermal performance of the optimized wall is clearly effective. This is attributed to the properties of the insulation used: low thermal conductivity and high relative density compared to conventional materials, which are ideal for cold climates. Such performance eliminates the need for additional strategies, such as phase change materials, multilayer composite systems, or supplemental insulation reinforcements [63,64].

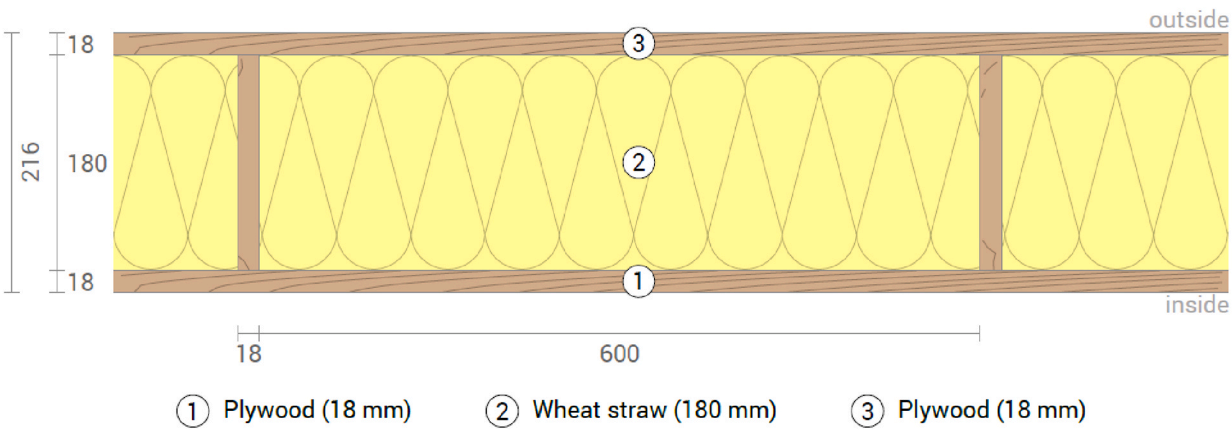

Fig. 5. Materials and thicknesses of the optimized industrialized construction system.

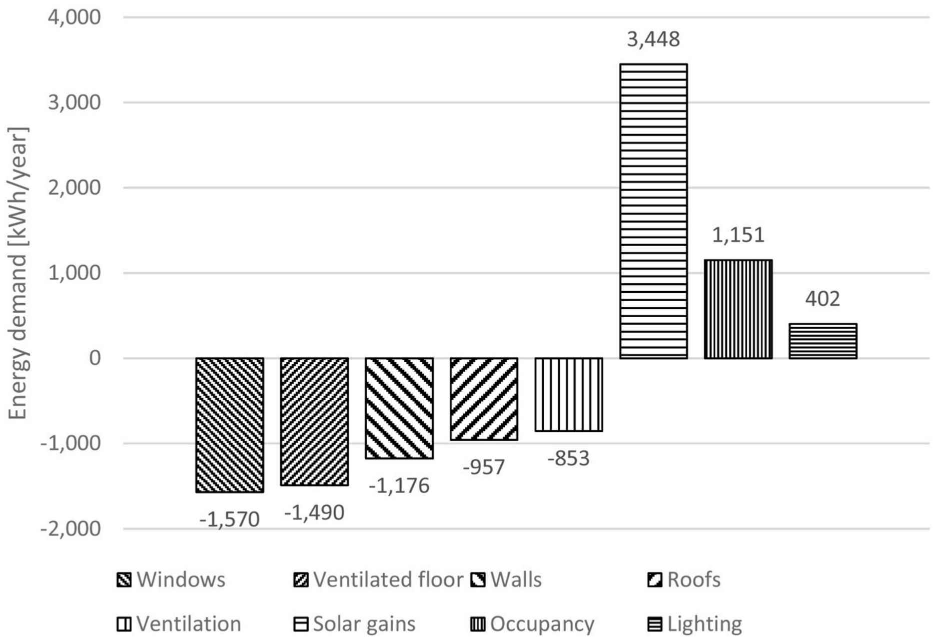

Fig. 6. Energy balance; losses and gains of the dwelling.

Compared to retrofitting strategies, which can achieve up to 17 % reductions in energy demand with investment paybacks of 3–4 years, these results suggest that early-stage design interventions, particularly in the selection of wall insulation, can be more effective and sustainable [65,66].

Regarding energy gains, the main contribution comes from direct solar radiation, with 3448 [kWh/year], equivalent to 69 % of total gains. This is followed by internal heat gains from occupants, with 1151 [kWh/year] (23 %), and lighting, with 402 [kWh/year] (8 %).

3.2.2. Carbon footprint and costs

The total carbon footprint of the dwelling, considering emissions associated with material extraction and transport, as well as the annual operational phase under the optimized industrialized construction system, was 5207 [$kgCO_2eq$/year]. Normalized by surface area, this equals 82.6 [$kgCO_2eq/m^2$year], which is almost three times lower than that of homes built with traditional systems [67,68], and up to five times lower compared to the maximum benchmark values established by some countries as future reference limits [69,70]. However, when compared to a house built with CLT panels and a fully upgraded envelope, the case study's footprint is almost seven times higher [71]. This difference is partly explained by the assumption of a fully electric resistance heating system operating with an efficiency (η) of 1.0, representative of direct electricity-to-heat conversion. When considering a more realistic scenario with an electric heat pump (CoP = 3), operational emissions would decrease by approximately 66 %, resulting in a total carbon footprint of about 1740 [$kgCO_2eq$/year] (equivalent to 27.5 [$kgCO_2eq/m^2$·year]). Under this condition, the environmental performance of the proposed system would approach that of CLT-based buildings, reinforcing its potential as a low-carbon and energy-efficient construction solution for affordable housing in cold-climate regions.

It is important to emphasize that comparison with CLT buildings should be interpreted considering the different construction typologies and system boundaries considered. While CLT houses tend to show lower operational emissions due to their higher insulation levels and integrated design, the proposed system achieves comparable environmental performance under realistic CoP values, using simpler manufacturing processes and locally available bio-based materials. Therefore, the results highlight the potential for achieving low-carbon outcomes through accessible and replicable industrialized systems, even when compared to high-performance technologies such as CLT.

In this context, various studies have noted that combining industrialized construction, wood-based systems, and residual materials, along with digital planning tools, can substantially reduce the carbon footprint compared to concrete or steel-based systems. For instance, a Chilean study comparing lightweight timber-frame houses with solid wood houses found that the latter emitted an additional 2519 [$kgCO_2eq$] during the extraction, production, transport, and assembly phases [72]. This finding aligns with others that highlight that although wood has high carbon storage potential, its initial emissions may exceed those of conventional lightweight systems [73,74]. Therefore, material selection must be carefully evaluated based on project type, geographic location, and construction context [75,76].

As for total construction cost, the industrialized solution reached a value of USD 58,847. This amount falls within the eligible subsidy range for brackets 2 and 3 of the Chilean housing program for middle-income families. However, this cost still represents a barrier for direct application in lower-income segments (C1b to E), illustrating the structural challenge of balancing sustainability and affordability. Economic feasibility studies have shown that while using local and natural materials (such as lightweight quincha systems) can reduce environmental impact, initial costs tend to increase due to the need for specialized training and limited availability of materials in certain regions [77,78]. This has also been reported in other studies, which warn that implementing industrialized systems may have the opposite effect, increase final housing costs if not plan holistically [79].

3.2.3. Assembly and disassembly time

Fig. 7 shows the student group during the assembly test, specifically during the manual review phase (a) and the full-scale laboratory wall assembly (b).

Table 4 summarizes the results of the first attempt at assembling and disassembling the wall module, recording for each group the manual reading time, number of restarts, total assembly time, and perceived difficulty.

The group that achieved the shortest assembly time was Group 1, with 9 min and 45 s, after reading the manual twice. In contrast, Group 3 recorded the longest time (45 min), with two restarts and three manual readings. Although all teams reported low difficulty in understanding the manual, the assembly process was generally evaluated as moderately difficult. A common observation was that some pieces did not fit easily, which was attributed to moisture absorption during storage, causing expansion of 1–2 [mm] in certain connection areas.

The disassembly process was considerably faster, with an average of 35 s, and was described as simple, although participants noted that some joints could break if too much force was applied.

During the second attempt, summarized in Table 5, all groups significantly improved their time. Group 4 achieved the best result with 1 min and 50 s, and Group 3 reduced its time by 90 % compared to the first attempt. Only two groups briefly reviewed the manual, and all agreed that once the assembly logic was understood, the process became much smoother. The teams highlighted the importance of collaborative work, focused effort, and the use of support tools such as rubber mallets to facilitate the fitting of slightly deformed parts. Additionally, the wooden components showed stable dimensional behavior under the controlled indoor conditions of the test, confirming the adequacy of the 1–2 mm tolerance considered during design and CNC cutting. In practical applications, however, proper storage and humidity control are essential, since moisture uptake may alter panel dimensions and affect joint precision [80].

The time reduction between the first and second assembly attempts shows that this system features a rapid learning curve. This is due in part to the fact that it does not require mechanical fasteners but is instead based on a fully plywood-based design with precisely interlocking components. Therefore, material quality and storage conditions are key to maintaining assembly efficiency. Moreover, the joint design facilitates an intuitive process, reinforcing the potential of this system for accelerated construction [81]. Nevertheless, these findings should be interpreted as exploratory evidence of assembly efficiency and learning potential, rather than conclusive indicators of large-scale productivity. Future validation with professional construction teams under real site conditions will be necessary to confirm these trends. However, it is important to note that other industrialized systems requiring metal connectors or external components must address criteria such as connection type, accessibility, component independence, and disassembly without damage [82]. In this regard, various studies recommend that disassembly strategies be integrated from the early stages, alongside energy and life cycle analyses. Tools like Building Information Modeling (BIM) are fundamental for advancing toward construction systems aligned with circular economy models [83].

At the projection level, it was estimated that the case study dwelling would require 64 wall modules, equivalent to 128 plywood panels. According to previous studies [10], cutting these pieces with a CNC machine would take approximately 85 h, which equates to 11 working days under 8-h shifts. Assuming a conservative average assembly time of 4 min per block, the complete structural assembly of the walls would take approximately 4.3 h, or half a working day with a single team. In total, the cutting and wall assembly process, under a conservative scenario with one CNC machine and one team, would require around 12 working days.

Extending this projection to the other structural components (floor: 11 days; roof: 10 days), the complete structural shell of the dwelling could be assembled in about 33 days. It is important to note that these estimates refer exclusively to the structural phase and

Fig. 7. Student group in the process of wall assembly (a) and installation in laboratory prototype (b).

Table 4
Details of the wall assembly and disassembly process, first attempt.

Group	Manual Reading time [min]	Times the manual was read	Manual difficulty (1–5)	Times the assembly was restarted	Time from start to restart [min]	Total assembly time [min]	Assembly difficulty (1–5)
1	1:00	2	1	–	–	9:45	3
2	0:30	3	1	1	20:00	25:00	5
3	0:16	3	1	2	4:00	45:00	2
4	0:41	1	1	1	2:00	11:35	2
5	0:21	1	2	–	–	12:00	3

Table 5
Details of the wall assembly and disassembly process, second attempt.

Group	Manual Reading time [min]	Times the manual was read	Manual difficulty (1–5)	Times the assembly was restarted	Time from start to restart [min]	Total assembly time [min]	Assembly difficulty (1–5)
1	0	0	1	0	0	2:25	3
2	0:20	1	1	0	0	3:15	3
3	0:20	1	1	0	0	4:15	2
4	0	0	1	0	0	1:50	1
5	0:20	1	1	0	0	3:00	1

exclude installations, finishes, and insulation application. Under this condition, the structural assembly rate of the system reaches 1.9 [m^2/day], which is nearly eight times faster than the national average for conventional systems in Chile and approximately five times faster than the average reported for OECD countries [84]. Furthermore, if a second CNC machine and a second assembly line were incorporated, the rate could increase to 3.8 [m^2/day], exceeding the 3.3 [m^2/day] minimum estimated as necessary to address the housing deficit in several Latin American countries, including Chile (approximately 600,000 homes) within four years [85]. These figures should be interpreted as indicative of potential structural assembly efficiency, rather than as comprehensive productivity metrics for full construction workflows.

4. Conclusions

The study demonstrated that the proposed optimization methodology effectively integrates environmental, economic, and constructive performance criteria to support decision-making in industrialized construction. The optimized modular wall system achieved simultaneous improvements in energy efficiency, carbon footprint, and cost compared with a traditional wall configuration. Under realistic operational assumptions using a heat pump (CoP = 3), the total carbon footprint of the dwelling decreases by approximately 66 %, highlighting the relevance of operational efficiency in environmental assessments.

The findings also confirm that industrialized construction can significantly improve project efficiency by simplifying assembly processes and reducing construction time. Under controlled test conditions, the modular wall system achieved assembly rates up to eight times faster than conventional methods, illustrating its potential to accelerate construction without compromising quality.

Furthermore, the modular system exhibited practical advantages such as ease of assembly and disassembly, reusability of components, and compatibility with parametric design and digital fabrication tools—key aspects of circular construction. These results contribute to the advancement of sustainable and replicable housing solutions, particularly for cold-climate regions where reducing energy demand and construction costs remains a critical challenge.

Overall, the study provides evidence that the integration of multi-objective optimization with industrialized and bio-based systems offers a robust pathway toward more efficient, low-carbon, and scalable construction strategies.

CRediT authorship contribution statement

Carlos Rojas-Herrera: Writing – original draft, Methodology, Investigation, Formal analysis, Conceptualization. **Aner Martínez-Soto:** Writing – review & editing, Validation. **Rafael Batres:** Writing – original draft, Methodology. **Rodrigo Cancino Carrasco:** Writing – review & editing, Supervision. **Natalia Reyes Barbato:** Writing – review & editing, Supervision.

Informed consent statement

Not applicable.

Institutional review board statement

Not applicable.

Funding

This research received no external funding.

Declaration of competing interest

The authors declare that they have no known competing financial interests or personal relationships that could have appeared to influence the work reported in this paper.

Acknowledgments

The authors would like to thank Rayen Vallejos, Javiera Vasconcello, and the group of students and faculty members from the Construction Engineering at Universidad Autónoma de Chile, Temuco, for their valuable participation and support in the energy modeling and assembly of the construction elements.

APPENDIX A. – Configuration and input data of the simulation model and envelope assemblies

This appendix presents the detailed composition of each construction element used in the case study dwelling, including materials, thicknesses, and corresponding thermal transmittance (U-values). The configurations were defined according to validated solutions from various Atmospheric Decontamination Plans (PDA) issued by the Chilean Ministerio del Medio Ambiente and officially approved by the Ministerio de Vivienda y Urbanismo (MINVU). These details include the traditional wall used as a reference case, as well as the roof, ventilated floor, windows, and doors, ensuring regulatory compliance for the studied cold-climate zone.

1. Model input parameters

- Occupancy density: The dwelling was designed to accommodate a maximum of five people, distributed across two double bedrooms and one single room. Based on this, the occupancy density was calculated as 0.0794 [persons/m^2].
- Occupancy schedules: Occupancy profiles were defined using the default circulation templates provided by the energy simulation software, applied to residential spaces such as bedrooms, living-dining areas, kitchens, and bathrooms [29].
- Design temperaturas: Setpoint temperatures were defined according to occupant thermal comfort requirements. During occupied periods, heating and cooling setpoints of 20 °C and 24 °C were used, respectively. For unoccupied periods, the software's secondary setpoints were applied: 12 °C for heating and 28 °C for cooling [30,31].
- Lighting: The lighting load was calculated based on a system of 12 LED luminaires, each rated at 9.5 W, distributed throughout the dwelling's habitable areas. The total estimated load was 1.81 [W/m^2], primarily assigned to nighttime occupancy periods [32].
- Ventilation: The minimum required ventilation rate was calculated according to Chilean Standard NCh3309:2014, using the following equation (A1):

$$Qtotal = 0.015 \times Afloor + 3.5\,(Nbr + 1) \tag{A1}$$

where *Qtotal* is the ventilation rate in liters per second [l/s], *Afloor* is the useable floor area in square meters, and *Nbr* is the number of bedrooms. For 63 [m^2] home with three bedrooms, the calculated ventilation rate was 14.95 [l/s], equivalent to 0.378 air changes per hour (ACh) for the total volume of the dwelling. This value was entered as a global building-level input and distributed across each space.

-Air infiltration: The air infiltration rate was set to 5 [ACH], in accordance with the updated Chilean thermal regulation for the studied climate zone. In the simulation model, this corresponds to a global infiltration flow of 0.196 [m^3/s] at the building level.

2. Envelope assemblies

- Traditional wall (reference): Solution F9 from the PDA of Temuco and Padre Las Casas ("Timber stud wall with internal insulation and external EIFS system"). From interior to exterior: 10 [mm] gypsum board, 2 × 4″ pine stud frame, 90 [mm] EPS (density: 30 [kg/m^3]), 11.1 [mm] plywood panel, and a second 40 [mm] EPS layer (same density). Total thermal transmittance: 0.292 [W/m^{2}K].

- Roof: Solution F10 from the Osorno PDA ("Roof truss with fiberglass insulation over ceiling"). From interior to exterior: 10 [mm] gypsum board, 2 × 2″ pine framing, and 160 [mm] fiberglass insulation. Thermal transmittance: 0.25 [W/m^{2}K].
- Ventilated floor: Solution F14 from the Osorno PDA ("Double expanded polystyrene insulation"). Layers: 18 [mm] plywood panel, vapor barrier, 50 [mm] EPS (density: [15 kg/m^3]), 2 × 6″ pine joists, additional 80 [mm] EPS (same density), moisture barrier, and 6 [mm] fiber-cement exterior finish. Thermal transmittance: 0.32 [W/m^{2}K].
- Windows: Double-glazed sealed units (two 4 [mm] panes separated by a 12 [mm] air gap) with PVC frames. Thermal transmittance: 2.80 [W/m^{2}K].
- Doors: Solid wood, 45 [mm] thick. Thermal transmittance: 1.70 [W/m^{2}K].

Table A1
Details of materials and thicknesses of the dwelling's building elements.

Building Element	Material	Thickness [mm]	Thermal Transmittance [W/m2K]
Modular Wall	Plywood	18	0.288
	Thermal Insulation:		
	a) Sawdust	150–250	
	b) Wheat Straw	110–250	
	c) Fiberglass	130–250	
	Plywood	18–30	
Traditional Wall	Plasterboard	10	0.290
	Pine IPV 2 × 4″	90	
	Expanded Polystyrene	90	
	Plywood	11.1	
	Expanded Polystyrene (EIFS)	40	
Roof	Plasterboard	10	0.250
	Pine IPV 2 × 2″	45	
	Fiberglass	160	
Ventilated Floor	Plywood	18	0.320
	Vapor Barrier	0.2	
	Expanded Polystyrene	50	
	Pine IPV 2 × 6″	150	
	Expanded Polystyrene	80	
	Moisture Barrier	0.37	
	Fibercement	6	
Windows	Glass	4	2.80
	Air gap	12	
	Glass	4	
Doors	Solid Wood	45	1.70

APPENDIX B. – Background of materials used in the energy simulation/optimization

1. Costs

Table B1
Plywood board cost

Thickness [mm]	Dimensions [m]		Yield [m^2]	Costs [USD]	
	Width	Height		Total	Unitary [USD/m^2]
18	1.22	2.44	2.98	24.17	8.12
21	1.20	2.40	2.88	28.77	9.99
25	1.22	2.44	2.98	29.96	10.06
30	1.22	2.44	2.98	40.95	13.62

Table B2
Sawdust cost

Thickness [m]	Density [kg/m^3]	Cost [USD/kg]	Cost [USD/m^2]
0.15	124	0.34	6.38
0.16			6.81
0.17			7.23
0.18			7.66
0.19			8.09
0.20			8.51
0.21			8.93
0.22			9.36
0.23			9.79
0.24			10.22
0.25			10.64

Table B3
Wheat Straw cost

Thickness [m]	Density [kg/m^3]	Cost [USD/kg]	Cost [USD/m^2]
0.11	81	0.28	2.50
0.12			2.72
0.13			2.95
0.14			3.18
0.15			3.41
0.16			3.63
0.17			3.86
0.18			4.09
0.19			4.31
0.20			4.54
0.21			4.77
0.22			4.99
0.23			5.22
0.24			5.45
0.25			5.67

Table B4
Glass wool cost

Thickness [mm]	Dimensions [m]		Yield [m^2]	Costs [USD]	
	Width	Height		Total	Unitary [USD/m^2]
40	1.2	24	28.8	46.31	1.61
50	1.2	24	28.8	72.76	2.53
60	1.2	12	14.4	55.62	3.86
80	1.2	8.33	9.9	45.68	4.57
100	1.2	7.5	9	63.44	7.05
120	1.2	7.5	9	68.99	7.66
140	1.2	7.5	9	52.31	5.81
160	1.2	5	6	45.26	7.54

2. Carbon footprint

Table B5
Carbon footprint of materials

Material	[kg CO_2eq]	[kg CO_2eq/kg]
OSB	192	0.30
Plywood board	33.2	0.06
Gypsum board	2.52	0.21
Sawdust	26.5	0.13
EPS	5.05	0.17
Glass wool	1.08	1.80
Wheat straw	10.3	0.10

APPENDIX C. – Modular wall assembly manual

1. Identification of pieces.

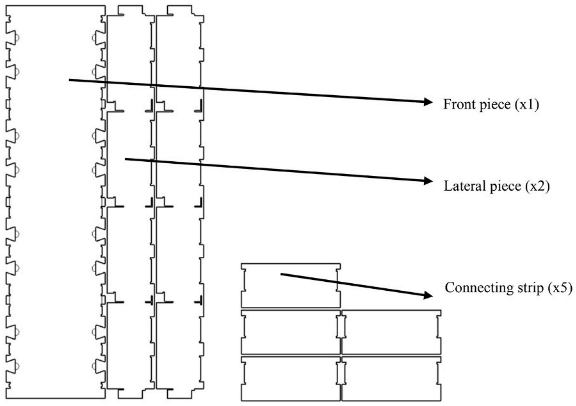

1. Assembly instructions.

- Place one lateral piece on the floor, on a flat surface.

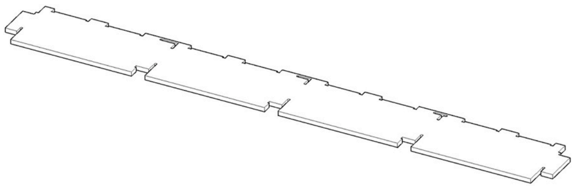

- Insert the wall cap into the lateral piece, ensuring all the tabs fit correctly. Make sure the notches of the ties (see detail) are oriented outward from the wall module.

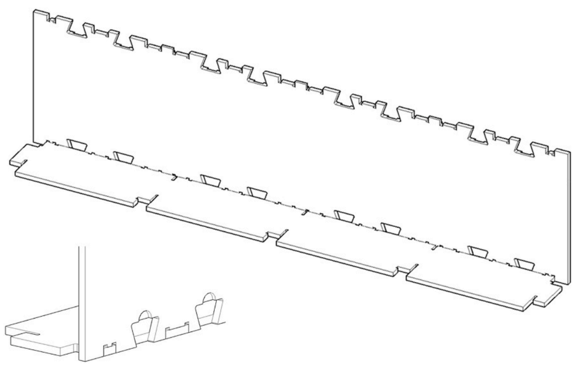

- Insert the five connecting strips into the lateral piece.

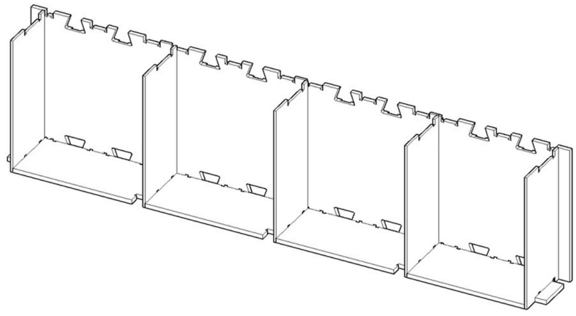

- Insert the other lateral piece of the module, following the same direction as the first lateral piece, ensuring that both the tabs of the cap and the tabs of the connecting strips align properly.

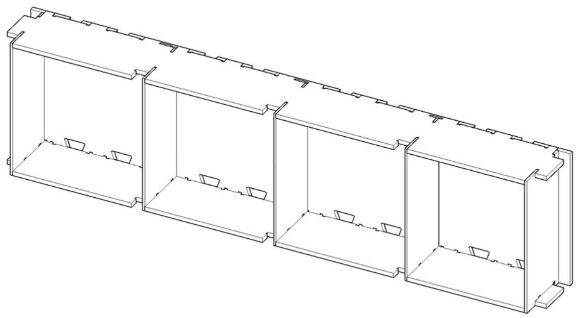

- Firmly press the pieces together to ensure proper assembly. Use a hammer or similar tool if necessary. To ensure the stability of the wall module, screws of 1 ¼" can be placed along the lateral sides of the wall to secure the pieces.

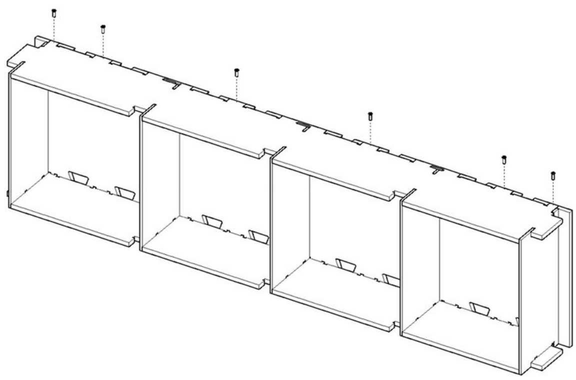

Data availability

Data will be made available on request.

References

[1] M. Almeida, F. Ascione, T. Iovane, M. Mastellone, R. Mateus, Impact of life cycle assessment analysis on energy efficiency projects in Mediterranean residential buildings, Energy 295 (2024) 130994, https://doi.org/10.1016/J.ENERGY.2024.130994.

[2] C. Rojas, K. Rodriguez, J.P. Cárdenas-R, Evaluation of two Chilean Native Macroalgae: "pelillo" (Gracilaria chilensis) and "Lamilla" (Ulva sp.) for Thermal Insulation Application, Buildings 13 (2023), https://doi.org/10.3390/buildings13102622.

[3] F. Ascione, N. Bianco, C. De Stasio, G.M. Mauro, G.P. Vanoli, A new methodology for cost-optimal analysis by means of the multi-objective optimization of building energy performance, Energy Build. 88 (2015) 78–90, https://doi.org/10.1016/J.ENBUILD.2014.11.058.

[4] L. Larrea-Sáez, C. Cuevas, Y. Casas-Ledón, Energy and environmental assessment of the chilean social housing: effect of insulation materials and climates, J. Clean. Prod. 392 (2023) 136234, https://doi.org/10.1016/J.JCLEPRO.2023.136234.

[5] A. Tapia-Calderón, D. Boer, C. Salinas-Lira, D.A. Vasco, Optimized thermal envelope of low-income dwellings in Santiago de Chile incorporating Pinus radiata wood impregnated with phase change materials, J. Energy Storage 60 (2023) 106665, https://doi.org/10.1016/J.EST.2023.106665.

[6] C. Rojas-Herrera, J.P. Cárdenas-R, M. Soto-Acuña, Physical characterization of two Native Chilean Macroalgae: Luga (Sarcothalia crispata) and Sargazo (Sargassum) for their use as thermal insulation material in sustainable housing, Advances in Bio-Based Materials for Construction and Energy Efficiency (2025) 499–511, https://doi.org/10.1016/B978-0-443-32800-8.00001-9.

[7] S.B. Sadineni, S. Madala, R.F. Boehm, Passive building energy savings: a review of building envelope components, Renew. Sustain. Energy Rev. 15 (2011) 3617–3631, https://doi.org/10.1016/J.RSER.2011.07.014.

[8] U. Kınay, A. Laukkarinen, J. Vinha, Renovation wave of the residential building stock targets for the carbon-neutral: evaluation by Finland and Türkiye case studies for energy demand, Energy Sustain. Dev. 75 (2023) 1–24, https://doi.org/10.1016/J.ESD.2023.04.014.

[9] C. Rojas, K. Rodriguez, J.P. Cárdenas-R, Valorization of wheat crop waste in Araucanía, Chile: blowing technique and geographical analysis, Buildings 13 (2023), https://doi.org/10.3390/buildings13051152.

[10] C. Rojas-Herrera, A. Martínez-Soto, C. Avendaño-Vera, J.P. Cárdenas-R, Characterization and utilization of sawdust waste generated from advanced manufacture for its application as a thermal insulation in sustainable buildings using the blowing technique, J. Build. Eng. 88 (2024), https://doi.org/10.1016/j.jobe.2024.109217.

[11] K. Rodríguez Neira, C.J. Rojas-Herrera, J.P. Cárdenas-Ramírez, J. Torres Ramo, A. Sánchez-Ostiz, Characterization and energy performance of rice husk fiber insulation applied by the blowing technique in an industrialized modular housing system, Appl. Sci. 15 (2025), https://doi.org/10.3390/app15094602.

[12] M. Aravena, L. Almonacid-Muñoz, C. Rojas-Herrera, H. Herrera, J.P. Cárdenas-Ramírez, A. Veliz Reyes, C. Sagredo-Saez, Evaluation of the thermal insulation potential of post-harvest blocks using the native strain of the edible mushroom Pleurotus ostreatus, Buildings 14 (2024) 1–13, https://doi.org/10.3390/buildings14123908.

[13] F. Greer, A. Horvath, Modular construction's capacity to reduce embodied carbon emissions in California's housing sector, Build. Environ. 240 (2023) 110432, https://doi.org/10.1016/J.BUILDENV.2023.110432.

[14] C. Rojas-Herrera, A. Martínez-soto, C. Avendaño-vera, R.C. Carrasco, Industrialized construction : a systematic review of its benefits and guidelines for the development of new constructive solutions applied in sustainable projects, Appl. Sci. (2025) 1–30.

[15] F. Espino-González, M.E. Armas-Cabrera, F. Montesdeoca-Martínez, S. Velázquez-Medina, Optimization of energy consumption in residential housing within the framework of energy sustainability strategies. A case study in the Canary Islands, J. Build. Eng. 94 (2024) 110014, https://doi.org/10.1016/J.JOBE.2024.110014.

[16] Z. Zhan, P. Xia, D. Xia, Y. Hu, Multi-objective optimization in the construction of steel-concrete composite columns with carbon emission considerations: pareto front development and decision-making, Ain Shams Eng. J. 16 (2025) 103283, https://doi.org/10.1016/J.ASEJ.2025.103283.

[17] J. Wang, Z. Wang, H. Liu, Multi-objective stochastic time-cost-quality optimization for construction projects based on the reliability theory, KSCE J. Civ. Eng. 27 (2023) 4545–4556, https://doi.org/10.1007/S12205-023-1083-Z.

[18] Q. Gong, W. Ding, X. Liu, Y. Zeng, E. Adu, H. Shao, Multi-objective optimization framework for the building envelope of public rental housing in China's cold regions, J. Build. Eng. 104 (2025) 112261, https://doi.org/10.1016/J.JOBE.2025.112261.

[19] L. Xie, T. Chen, N. Joshi, Z. Li, Climate-responsive retrofitting strategy of elderly housing: health impacts based on data-driven multi-objective optimization of building envelopes, Build. Environ. 285 (2025) 113554, https://doi.org/10.1016/J.BUILDENV.2025.113554.

[20] P.E. Camporeale, M. del P. Mercader Moyano, J.D. Czajkowski, Multi-objective optimisation model: a housing block retrofit in Seville, Energy Build. 153 (2017) 476–484, https://doi.org/10.1016/J.ENBUILD.2017.08.023.

[21] K. Jeong, T. Hong, J. Kim, K. Cho, Development of a multi-objective optimization model for determining the optimal CO2 emissions reduction strategies for a multi-family housing complex, Renew. Sustain. Energy Rev. 110 (2019) 118–131, https://doi.org/10.1016/J.RSER.2019.04.068.

[22] N.M. Castrejon-Esparza, M.E. González-Trevizo, K.E. Martínez-Torres, M. Santamouris, Optimizing urban morphology: evolutionary design and multi-objective optimization of thermal comfort and energy performance-based city forms for microclimate adaptation, Energy Build. 342 (2025) 115750, https://doi.org/10.1016/J.ENBUILD.2025.115750.

[23] D. Esenarro, E. Porras, H. Ventura, J. Figueroa, V. Raymundo, L. Castañeda, Use of digital tools (Wikihouse System) in multi-local social housing, Sustainability 16 (2024), https://doi.org/10.3390/su16083231.

[24] WikiHouse, Blocks Wikihouse - Skylark 200, 2023.

[25] A. Martinez-Soto, M. Iannantuono, P. Macaya-Vitali, E. Nix, Towards low-carbon housing in Chile: optimisation and life cycle analysis of energy-efficient solutions, Case Stud. Therm. Eng. 28 (2021) 101579, https://doi.org/10.1016/J.CSITE.2021.101579.

[26] W. Li, Z. Zhou, Y. Han, An actual-performance-oriented study on the relationship between environmental efficiency and passive design factors for multi-family dwellings in cold areas, Energy Build. 285 (2023) 112825, https://doi.org/10.1016/J.ENBUILD.2023.112825.

[27] G. Yao, X. Guo, Z. Qian, Y. Pang, Y. Zhang, C. Xie, Application of thermal buffer spaces in the renovation of rural dwellings for nearly zero energy consumption in severe cold regions of China, J. Build. Eng. 99 (2025) 111543, https://doi.org/10.1016/J.JOBE.2024.111543.

[28] M.C. Peel, B.L. Finlayson, T.A. McMahon, Updated world map of the Köppen-Geiger climate classification, Hydrol. Earth Syst. Sci. 11 (2007) 1633–1644, https://doi.org/10.5194/hess-11-1633-2007.

[29] D. Sood, I. Alhindawi, U. Ali, D. Finn, J.A. McGrath, M.A. Byrne, J. O'Donnell, Zone-wise occupancy schedules developed using Time Use Survey data for building energy performance simulations, Data Brief 49 (2023) 109453, https://doi.org/10.1016/J.DIB.2023.109453.

[30] M. Serikawa, M. Satoh, W. Umishio, S. Kawakubo, J. Nakano, T. Akimoto, T. Ikaga, S. Murakami, Quantitative evaluation of the contributions of improved housing performances toward delivering sustainable development goals by a building energy simulation tool, Sustain. Cities Soc. 79 (2022) 103701, https://doi.org/10.1016/J.SCS.2022.103701.

[31] L. Larrea-Sáez, E. Muñoz, C. Cuevas, Y. Casas-Ledón, Optimizing insulation and heating systems for social housing in Chile: insights for sustainable energy policies, Energy 290 (2024) 130024, https://doi.org/10.1016/J.ENERGY.2023.130024.

[32] M. Zafari Jurshari, M. Yousefi Tazakor, M. Yeganeh, Optimizing the dimensional ratio and orientation of residential buildings in the humid temperate climate to reduce energy consumption (Case: rasht Iran), Case Stud. Therm. Eng. 59 (2024) 104484, https://doi.org/10.1016/J.CSITE.2024.104484.

[33] V. Gupta, C. Deb, Envelope design for low-energy buildings in the tropics: a review, Renew. Sustain. Energy Rev. 186 (2023) 113650, https://doi.org/10.1016/J.RSER.2023.113650.

[34] G. Sousa, B.M. Jones, P.A. Mirzaei, D. Robinson, A review and critique of UK housing stock energy models, modelling approaches and data sources, Energy Build. 151 (2017) 66–80, https://doi.org/10.1016/J.ENBUILD.2017.06.043.

[35] J. Zhang, L. Zhang, P. Ren, W. Hao, A. Xu, Multi-objective optimization prediction model for building parameters of photovoltaic windows based on NSGA II-BP, Case Stud. Therm. Eng. 64 (2024) 105500, https://doi.org/10.1016/J.CSITE.2024.105500.

[36] F. Zahra Benaddi, L. Boukhattem, P. Cesar Tabares-Velasco, Multi-objective optimization of building envelope components based on economic, environmental, and thermal comfort criteria, Energy Build. 305 (2024) 113909, https://doi.org/10.1016/J.ENBUILD.2024.113909.

[37] A. Ciardiello, F. Rosso, J. Dell'Olmo, V. Ciancio, M. Ferrero, F. Salata, Multi-objective approach to the optimization of shape and envelope in building energy design, Appl. Energy 280 (2020) 115984, https://doi.org/10.1016/J.APENERGY.2020.115984.
[38] R. Dash, , J.R. K., M. Fathima, , A. L., A. Mahapatro, M.L. Kolhe, Optimizing combined heat and power systems for multi-residential buildings: a multi-objective framework for sustainable energy management, J. Energy Storage 102 (2024) 113972, https://doi.org/10.1016/J.EST.2024.113972.
[39] J. Dou, X. Wang, Z. Liu, Q. Sun, X. Wang, J. He, Towards Pareto-optimal energy management in integrated energy systems: a multi-agent and multi-objective deep reinforcement learning approach, Int. J. Electr. Power Energy Syst. 159 (2024) 110022, https://doi.org/10.1016/J.IJEPES.2024.110022.
[40] M. Ibrahim, F. Harkouss, P. Biwole, F. Fardoun, S.E. Ouldboukhitine, Multi-objective hyperparameter optimization of artificial neural network in emulating building energy simulation, Energy Build. 337 (2025) 115643, https://doi.org/10.1016/J.ENBUILD.2025.115643.
[41] F.S. Arison, T. Tokumasu, Sholahudin, A.S. Yatim, N. Nasruddin, Multi-Objective optimization of TAF systems: enhancing air cleanliness and energy efficiency in surgical environments, Build. Environ. 279 (2025) 112977, https://doi.org/10.1016/J.BUILDENV.2025.112977.
[42] R.H. Stewart, T.S. Palmer, B. DuPont, A survey of multi-objective optimization methods and their applications for nuclear scientists and engineers, Prog. Nucl. Energy 138 (2021) 103830, https://doi.org/10.1016/J.PNUCENE.2021.103830.
[43] M. Zukowski, Multi-aspect analysis of measures to reduce the building's energy demand, J. Build. Eng. 91 (2024) 109758, https://doi.org/10.1016/J.JOBE.2024.109758.
[44] L. Ben-Alon, V. Loftness, K.A. Harries, E. Cochran Hameen, Life cycle assessment (LCA) of natural vs conventional building assemblies, Renew. Sustain. Energy Rev. 144 (2021) 110951, https://doi.org/10.1016/J.RSER.2021.110951.
[45] S.M.A. Hosseini, L. Farahzadi, O. Pons, Assessing the sustainability index of different post-disaster temporary housing unit configuration types, J. Build. Eng. 42 (2021) 102806, https://doi.org/10.1016/J.JOBE.2021.102806.
[46] L. Sun, Z. Hu, M. Mae, T. Imaizumi, A predictive COP model for air source heat pumps under extreme heat conditions using no experimental data, Energy Build. 339 (2025) 115749, https://doi.org/10.1016/J.ENBUILD.2025.115749.
[47] Y. Ji, J. Lv, H.X. Li, Y. Liu, F. Yao, X. Liu, S. Wang, Improving the performance of prefabricated houses through multi-objective optimization design, J. Build. Eng. 84 (2024) 108579, https://doi.org/10.1016/J.JOBE.2024.108579.
[48] B. Bueno, Factibilidad De Fabricación De Viviendas Con Sistema Wikihouse Para la Autoconstrucción En Chile: Entendimientos De Las Barreras Para la Autoconstrucción De Viviendas De Bajo Costo En El País Utilizando El Sistema constructivo open-source De Wikihouse Sky, Repositorio Académico, Universidad de Chile, 2022, https://doi.org/10.58011/eh9w-m987.
[49] X. Liang, X. Gu, M.M. Paing Hsu, Y. He, R. Zhang, C. Cai, Z. Wang, Design and development of composite plywood that integrates fire resistance, water resistance and wear resistance, J Renew Mater 11 (2023) 2333–2344, https://doi.org/10.32604/JRM.2023.026137.
[50] B.M. Tehrani, A. Alwisy, Streamlining design-to-manufacturing for assembly-based robotics in wood panel framing tasks of industrialized construction: introducing a BIM-to-BoT (B2B) framework, Adv. Eng. Inform. 65 (2025) 103393, https://doi.org/10.1016/J.AEI.2025.103393.
[51] G. Granello, T. Reynolds, C. Prest, Structural performance of composite WikiHouse beams from CNC-cut timber panels, Eng. Struct. 252 (2022) 113639, https://doi.org/10.1016/J.ENGSTRUCT.2021.113639.
[52] H. Kim, S. Chang, Developing energy usage strategies by optimizing residential setpoints for affordable and health-promoting energy consumption, Appl. Energy 394 (2025) 126127, https://doi.org/10.1016/J.APENERGY.2025.126127.
[53] A. Saleem, A.A. Badr, B.H. Alyas, O.R. Alomar, Performance of thermal insulation of different composite walls and roofs materials used for energy efficient building construction in Iraq, Frontiers in Heat and Mass Transfer 22 (2024) 1231–1244, https://doi.org/10.32604/FHMT.2024.053770.
[54] J. Sun, Q. Zhang, A. Chen, Z. Wu, Energy performance of buildings with multi-ribbed composite wall structural system, J. Build. Eng. 91 (2024) 109614, https://doi.org/10.1016/J.JOBE.2024.109614.
[55] K. Rodríguez Neira, J.P. Cárdenas-Ramírez, C.J. Rojas-Herrera, L. Haurie, A.M. Lacasta, J. Torres Ramo, A. Sánchez-Ostiz, Assessment of elaboration and performance of Rice Husk-Based thermal insulation material for building applications, Buildings 14 (2024) 1720, https://doi.org/10.3390/buildings14061720.
[56] A.W. Makhloufi, S. Louafi, Optimising building performance for a resilient future: a multi-objective approach to Net Zero energy strategies, Energy Build. 324 (2024) 114869, https://doi.org/10.1016/J.ENBUILD.2024.114869.
[57] A. Saleem, C.E. Ugalde-Loo, Thermal performance analysis of a heat pump-based energy system to meet heating and cooling demand of residential buildings, Appl. Energy 383 (2025) 125306, https://doi.org/10.1016/J.APENERGY.2025.125306.
[58] C. Zhang, M. Ullah, H. Alofaysan, H. Hakimov, S. Audrey, Modeling and managing residential energy demand for a low-carbon future, Energy Strategy Rev. 57 (2025) 101610, https://doi.org/10.1016/J.ESR.2024.101610.
[59] S. Ouanes, L. Sriti, Regression-based sensitivity analysis and multi-objective optimisation of energy performance and thermal comfort: building envelope design in hot arid urban context, Build. Environ. 248 (2024) 111099, https://doi.org/10.1016/J.BUILDENV.2023.111099.
[60] G.R. Araújo, R. Gomes, P. Ferrão, M.G. Gomes, Optimizing building retrofit through data analytics: a study of multi-objective optimization and surrogate models derived from energy performance certificates, Energy and Built Environment 5 (2024) 889–899, https://doi.org/10.1016/J.ENBENV.2023.07.002.
[61] Y. Shen, Y. Pan, BIM-supported automatic energy performance analysis for green building design using explainable machine learning and multi-objective optimization, Appl. Energy 333 (2023) 120575, https://doi.org/10.1016/J.APENERGY.2022.120575.
[62] G.R. Araújo, H. Teixeira, M.G. Gomes, A.M. Rodrigues, Multi-objective optimization of thermochromic glazing properties to enhance building energy performance, Sol. Energy 249 (2023) 446–456, https://doi.org/10.1016/J.SOLENER.2022.11.043.
[63] Y. Chen, Y. Sun, J. Yang, J. Tan, Y. Liu, D. ce Gao, Demand response with PCM-based pipe-embedded wall in commercial buildings: combined passive and active energy storage in envelopes, Energy 308 (2024) 132980, https://doi.org/10.1016/J.ENERGY.2024.132980.
[64] R. Ma, R. Ma, E. Long, Analysis of the rule of window-to-wall ratio on energy demand of residential buildings in different locations in China, Heliyon 9 (2023) e12803, https://doi.org/10.1016/J.HELIYON.2023.E12803.
[65] Z. Shen, D. Howard, D. Hun, S. Mumme, S. Shrestha, Coupling thermal energy storage with a thermally anisotropic building envelope for building demand-side management across various US climate conditions, Energy Build. 328 (2025) 115204, https://doi.org/10.1016/J.ENBUILD.2024.115204.
[66] A. Mustufa, M. Anwar, T.I. Khan, Energy optimization of an institutional building to reduce the energy and air conditioning demand, J. Build. Eng. 98 (2024) 111309, https://doi.org/10.1016/J.JOBE.2024.111309.
[67] B.L.E. de Lara, C.S.G. Penteado, Environmental assessment of construction waste prevention: a case study in a social housing project in Southeast Brazil, Cleaner Waste Systems 8 (2024) 100145, https://doi.org/10.1016/J.CLWAS.2024.100145.
[68] L.B. López-Sosa, A.Y. Oseguera-Rivera, M. Morales-Máximo, J.C. Corral-Huacuz, J.C.L. Valdespino, G.M. Rodríguez-Torres, M. Rivero, C.A. García, S. Orozco, Multivariate analysis of materials used in rural housing in Mexico considering sustainability indicators: towards suitable house construction, Results Eng. 25 (2025) 103744, https://doi.org/10.1016/J.RINENG.2024.103744.
[69] A.K. Santos, V.M. Ferreira, A.C. Dias, Promoting decarbonisation in the construction of new buildings: a strategy to calculate the Embodied Carbon Footprint, J. Build. Eng. 103 (2025) 112037, https://doi.org/10.1016/J.JOBE.2025.112037.
[70] C.Z. Li, V.W. Tam, M. Ma, S. Wen, Carbon emission analysis and multi-objective optimization of modular integrated construction using petri net simulation, Energy Build. 339 (2025) 115784, https://doi.org/10.1016/J.ENBUILD.2025.115784.
[71] Y. Kang, B.Y. Yun, S. Kim, Transformative enhancements in CLT housing: a three-step approach to minimizing energy consumption and carbon footprint, Energy Build. 329 (2025) 115275, https://doi.org/10.1016/J.ENBUILD.2025.115275.
[72] G. Venezian, María Catalina & Felmer, Análisis De La Huella De Carbono De La Construcción De Una Vivienda De Madera Tradicional Y Una Vivienda De Madera Masiva Para El Centro – Sur De Chile, Universidad de Chile. Facultad de Arquitectura y Urbanismo, 2022, p. 28.
[73] R.E. López-Guerrero, S. Vera, M. Carpio, A quantitative and qualitative evaluation of the sustainability of industrialised building systems: a bibliographic review and analysis of case studies, Renew. Sustain. Energy Rev. 157 (2022) 112034, https://doi.org/10.1016/J.RSER.2021.112034.
[74] C. Llatas, N. Bizcocho, B. Soust-Verdaguer, M.V. Montes, R. Quiñones, An LCA-based model for assessing prevention versus non-prevention of construction waste in buildings, Waste Manag. 126 (2021) 608–622, https://doi.org/10.1016/J.WASMAN.2021.03.047.

[75] M.J. Rukavina, D. Skejić, A. Kralj, T. Ščapec, B. Milovanović, Development of lightweight steel framed construction systems for nearly-zero energy buildings, Buildings 12 (2022), https://doi.org/10.3390/buildings12070929.
[76] K. Cai, H. Wang, J. Wang, J. Bai, J. Zuo, K. Chan, K. Lai, Q. Song, Mitigating lifecycle GHG emissions of building sector through prefabricated light-steel buildings in comparison with traditional cast-in-place buildings, Resour. Conserv. Recycl. 194 (2023) 107007, https://doi.org/10.1016/J.RESCONREC.2023.107007.
[77] P. Baquedano, R.R. Eudave, F.N. Miranda, S. Graus, T.M. Ferreira, Traditional earth construction in Latin America: a review on the construction systems and reinforcement strategies. Masonry Construction in Active Seismic Regions, 2021, pp. 99–121, https://doi.org/10.1016/B978-0-12-821087-1.00011-9.
[78] R. Acevedo Oliva, O.R. Carrillo Zúñiga, J. Broughton Weine, Construcción En Quincha Liviana, Ministerio de Vivienda y Urbanismo, 2017, p. 65. https://csustentable.minvu.gob.cl/wp-content/uploads/2020/03/CONSTRUCCION_CON_QUINCHA_LIVIANA_1a_edicion.pdf.
[79] E. Attouri, Z. Lafhaj, L. Ducoulombier, B. Linéatte, The current use of industrialized construction techniques in France: benefits, limits and future expectations, Clean Eng. Technol. 7 (2022) 100436, https://doi.org/10.1016/J.CLET.2022.100436.
[80] K. Zhang, R. Richman, Variability in moisture sorption isotherms of plywood and oriented strand board with accelerated ageing, Can. J. Civ. Eng. 48 (2020) 812–818, https://doi.org/10.1139/CJCE-2020-0249.
[81] G. Granello, T. Reynolds, C. Prest, Structural performance of composite WikiHouse beams from CNC-cut timber panels, Eng. Struct. 252 (2022) 113639, https://doi.org/10.1016/J.ENGSTRUCT.2021.113639.
[82] S. Attia, M. Al-Obaidy, M. Mori, C. Campain, E. Giannasi, M. van Vliet, E. Gasparri, Disassembly calculation criteria and methods for circular construction, Autom. ConStruct. 165 (2024) 105521, https://doi.org/10.1016/J.AUTCON.2024.105521.
[83] L.A. Akanbi, L.O. Oyedele, K. Omoteso, M. Bilal, O.O. Akinade, A.O. Ajayi, J.M. Davila Delgado, H.A. Owolabi, Disassembly and deconstruction analytics system (D-DAS) for construction in a circular economy, J. Clean. Prod. 223 (2019) 386–396, https://doi.org/10.1016/J.JCLEPRO.2019.03.172.
[84] L. Veas, H. Hernández, Estrategias público-privadas para el mejoramiento de la productividad en el sector de la construcción, Centro UC, Políticas Públicas, 21, https://politicaspublicas.uc.cl/publicacion/estrategias-publico-privadas-para-el-mejoramiento-de-la-productividad-en-el-sector-de-la-construccion/, 2023.
[85] S. Mendía, Análisis territorial de la brecha habitacional y el déficit potential comunal: Un insumo para el plan de emergencia habitacional, Urbanismo Social y Déficit Cero (2025) 1–45. Available at: https://urbanismosocial.cl/crisis-habitacional/.